Eur Spine J
DOI 10.1007/s00586-008-0828-1

ORIGINAL ARTICLE

Early stage disc degeneration does not have an appreciable affect on stiffness and load transfer following vertebroplasty and kyphoplasty

Victor Kosmopoulos · Tony S. Keller · Constantin Schizas

Received: 11 April 2008 / Revised: 31 October 2008 / Accepted: 3 November 2008

Abstract Vertebroplasty and kyphoplasty have been reported to alter the mechanical behavior of the treated and adjacent-level segments, and have been suggested to increase the risk for adjacent-level fractures. The intervertebral disc (IVD) plays an important role in the mechanical behavior of vertebral motion segments. Comparisons between normal and degenerative IVD motion segments following cement augmentation have yet to be reported. A microstructural finite element model of a degenerative IVD motion segment was constructed from micro-CT images. Microdamage within the vertebral body trabecular structure was used to simulate a slightly (I = 83.5% of intact stiffness), moderately (II = 57.8% of intact stiffness), and severely (III = 16.0% of intact stiffness) damaged motion segment. Six variable geometry single-segment cement repair strategies (models A–F) were studied at each damage level (I–III). IVD and bone stresses, and motion segment stiffness, were compared with the intact and baseline damage models (untreated), as well as, previous findings using normal IVD models with the same repair strategies. Overall, small differences were observed in motion segment stiffness and average stresses between the degenerative and normal disc repair models. We did however observe a reduction in endplate bulge and a redistribution in the microstructural tissue level stresses across both endplates and in the treated segment following early stage IVD degeneration. The cement augmentation strategy placing bone cement along the periphery of the vertebra (model E) proved to be the most advantageous in treating the degenerative IVD models by showing larger reductions in the average bone stresses (vertebral and endplate) as compared to the normal IVD models. Furthermore, only this repair strategy, and the complete cement fill strategy (model F), were able to restore the slightly damaged (I) motion segment stiffness above pre-damaged (intact) levels. Early stage IVD degeneration does not have an appreciable effect in motion segment stiffness and average stresses in the treated and adjacent-level segments following vertebroplasty and kyphoplasty. Placing bone cement in the periphery of the damaged vertebra in a degenerative IVD motion segment, minimizes load transfer, and may reduce the likelihood of adjacent-level fractures.

Keywords Load transfer · Vertebroplasty · Kyphoplasty · Microstructural finite element analysis · Vertebral motion segment

Dr. Tony S. Keller's life was tragically taken on the 6th of December 2006. Tony was a bright and energetic researcher, an outstanding teacher and mentor, and a beloved friend. He is greatly missed.

V. Kosmopoulos (✉) · T. S. Keller
Department of Orthopaedic Surgery,
Bone and Joint Research Center,
University of North Texas Health Science Center,
3400 Camp Bowie Boulevard (CBH 407),
Fort Worth, TX 76107, USA
e-mail: victor.kosmopoulos@yahoo.com

V. Kosmopoulos
Department of Orthopaedic Surgery, John Peter Smith Hospital,
Fort Worth, TX, USA

C. Schizas
Département de l'Appareil Locomoteur,
Centre Hospitalier Universitaire Vaudois,
The University of Lausanne, Lausanne, Switzerland

Introduction

When untreated, osteoporotic vertebral compression fractures (VCF) can result in chronic pain, progressive

Published online: 26 November 2008

kyphosis, and increased morbidity in the elderly [12, 17, 21, 22, 25–28]. Percutaneous vertebroplasty and kyphoplasty are two evolving, minimally invasive cement augmentation techniques for the treatment of VCFs. These procedures help to stabilize the collapsing vertebrae and relieve pain associated with VCFs [12, 21–23, 25, 27]. In addition, kyphoplasty has been associated with restoration of vertebral body (VB) height and spinal sagittal alignment [7, 21, 22, 25, 27–29]. An ongoing interest in researching these procedures has gained momentum from the suspicion that they may alter the mechanical behavior of the adjacent-level segment, leading to an increased risk for adjacent-level VCF [1, 3, 6, 12, 14, 27, 30].

Experimental and finite element (FE) numerical studies have shown that vertebral strength and stiffness can be restored to above normal levels in the augmented vertebrae [1, 2, 12, 17, 23, 30]. However, increased stiffness of the augmented segment is thought to increase the risk for adjacent-level VCF [1, 30]. Another view put forward is that the clinically observed increased risk for adjacent-level fracture is likely due to an already weakened adjacent segment, as was the case causing the initial fracture to the treated segment, naturally caused by systemic bone disease (e.g., osteoporosis) [37]. Furthermore, a recent study has suggested that indeed adjacent-level VCF are more likely following cement augmentation if full fracture reduction is not achieved [32]. The authors of this recent study report that a wedge-shaped fracture shifts the center of gravity anteriorly requiring a higher counteracting force by the erector spinae to re-establish balance. This elevated erector spinae force increases intradiscal pressure and endplate stresses far more than the cement augmentation itself [32]. Thus, from this point of view, adjacent segment fracture may originate from this increase in load as compared to an increase in vertebral stiffness following cement augmentation.

Finite element simulations have examined the efficacy of repair based on cement volume and distribution [12, 17, 23, 30] at different levels of bone damage and osteoporosis [12, 17, 30], the importance of bone cement material properties [17], and alterations in the load transfer behavior between vertebrae in a motion segment [1, 12, 30, 32, 37]. Advances in imaging (e.g., micro-computed tomography, μCT) together with dramatic improvements in computational power have allowed for the development of high-resolution, anatomically accurate, large-scale microstructural FE models. Unlike the more commonly used apparent FE modeling technique which idealizes the highly porous trabecular structure component of the vertebral centrum as a solid characterized in terms of its bulk or apparent density and modulus, microstructural FE models allow for precise discretization of the vertebral trabecular bone structure [16].

This study builds on previous research using microstructural FE models [11, 12, 15–19] to evaluate vertebral motion segment mechanical behavior and stress distributions following early stage intervertebral disc (IVD) degeneration. Previously, using a microstructural motion segment FE model with a normal IVD, cement augmentation was found to improve motion segment stiffness and substantially alter bone stress distributions in both the treated and adjacent-level vertebrae [12]. Results from such studies have shown that single segment partial fill cement augmentation strategies are effective in restoring motion segment stiffness to pre-damage levels for slightly damaged segments, but are ineffective in restoring stiffness for moderately and severely damaged segments [12, 17]. In the current study we hypothesize that early stage disc degeneration, shown to reduce motion segment stiffness [4, 5, 31], will considerably alter treated and adjacent-level stress distributions when compared to normal IVD segments following cement augmentation repair. Specifically this study aims to: (1) simulate trabecular bone damage in a thoracic motion segment (VB + degenerative IVD + VB); (2) evaluate repair of the damaged vertebrae using six different bone cement augmentation strategies; and (3) compare the novel results from this study using early stage IVD degeneration motion segment models with previous findings using normal IVD models. To our knowledge, this is the first study to compare a normal IVD to a degenerated IVD motion segment using multiple vertebroplasty and kyphoplasty treatment strategies.

Methods

A microstructural FE model of a motion segment used to simulate three bone damage levels and six polymethylmethacrylate (PMMA) augmentation strategies was adapted for use in this study [12]. Complete details of the microstructural FE model, including the numerical damage algorithm, and cement augmentation strategies are presented elsewhere [12, 16–19] and summarized below.

Finite element model

A 2.25-mm-thick, midsagittal thoracic (T7) μCT image from an elderly female (79 years of age) was used to construct an axi-symmetric, microstructural FE model of a thoracic motion segment. Trabecular bone tissue elements were modeled as isotropic, linear elastic, with an elastic modulus of 4,900 MPa and a Poisson's ratio (ν) of 0.3 [12, 16–19, 34]. Bone marrow elements ($E = 10$ kPa) and PMMA cement elements ($E = 2.16$ GPa) were assumed to have a Poisson's ratio of 0.3 [12, 16–19].

The healthy IVD nucleus and annulus regions were modeled as incompressible ($E = 1.0$ MPa, $v = 0.4999$) and slightly compressible ($E = 4.2$ MPa, $v = 0.45$), respectively [8, 12]. The nucleus and annulus geometries were representative of a thoracic IVD, wherein the nucleus occupied 32% of the total disc volume (nucleus + annulus) [12, 35]. Early stage disc degeneration was simulated by reducing the incompressibility and increasing the stiffness of the nucleus by assigning the same material properties to the nucleus as used for the annulus [10, 31, 33].

Damage simulations

To model damage within the VB trabecular bone structure, the microstructural FE motion segment model was combined with a validated iterative, element-by-element, modulus reducing microdamage algorithm [16, 18–20]. An axial compressive load was uniformly distributed and varied from 62.5 N to 1,000 N in 16 equal increments [12]. The degenerative IVD motion segment apparent modulus (stiffness) decreased from 144 MPa (intact undamaged stiffness) to 23.1 MPa at a load of 500 N (8th loading increment). The VB trabecular bone microdamage models associated with the sixth (83.5% of intact stiffness), seventh (57.8% of intact stiffness), and eighth (16.0% of intact stiffness) loading increments were used for the cement augmentation analyses described below. The three aforementioned damage models will be referred to as slightly damaged (I), moderately damaged (II), and severely or maximally damaged (III).

Cement augmentation strategies

In clinical practice, vertebroplasty cement augmentation involves forced injection of cement into the marrow spaces of the fractured VB. Vertebroplasty was simulated in this numerical study by replacing the superior VB segment's bone marrow elements with PMMA cement elements ($E = 2.16$ MPa, $v = 0.30$) [12, 17]. Kyphoplasty involves the insertion of a bone balloon into the VB using biplanar fluoroscopic image guidance. The balloon is inflated causing the adjacent trabecular bone to compact, and a cavity devoid of bone is created. PMMA cement is deposited into this cavity with more control and with less pressure as compared to vertebroplasty. To simulate kyphoplasty both the trabecular bone elements and bone marrow elements were replaced with PMMA cement elements [12]. This approach produces a PMMA-filled cavity devoid of bone but does not mimic the trabecular bone compaction that takes place clinically.

The same six PMMA cement augmentation strategies simulated using the normal IVD motion segment models were reproduced for this study. Each of the six augmentation strategies (models A–F) were used to repair each of the three damaged motion segment models (I–III) resulting in a total of 18 repair simulations (Fig. 1). Equivalent partial fill cement volume ($\sim$15% of the total VB volume) was modeled in five of the six augmentation strategies (models A–E). The last model was completely filled (model F) by replacing all the marrow elements with PMMA (55% of the total VB volume).

Analyses

Following damage, each of the cement augmentation repair models was subjected to a static compressive load with an apparent stress equivalent to that applied during the corresponding sixth, seventh, or eighth microdamage load iteration. von Mises stress distributions for both the superior and inferior VB segments and the IVD were computed from the element principal stresses. Load-sharing changes following cement augmentation in the endplate regions,

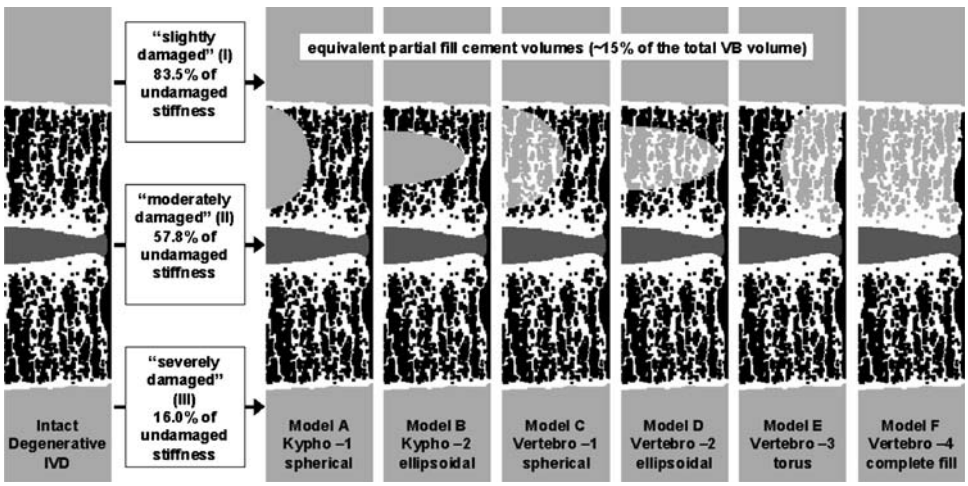

Fig. 1 An intact axi-symmetric degenerative IVD microstructural FE motion segment model (*left*) is evaluated at three bone damage levels (I, II, III) to determine the effectiveness of each of the six cement augmentation strategies (*models A–F*). PMMA cement in regions above and below the superior and inferior VBs was added to mimic in vitro experimental validation test conditions

5 mm above and below the IVD, were computed for the superior and inferior VBs. Results for each of the cement augmentation motion segment models were normalized with respect to either the corresponding intact or baseline damage untreated motion segment models to evaluate the effectiveness of each repair strategy. In addition, a focus was placed on comparing the cement augmented early stage disc degenerated motion segment models to the results previously reported using normal disc microstructural FE models [12]. In the presented normalized comparisons, positive percentile changes indicate an increase while negative changes indicate a decrease as compared with the intact, baseline damaged untreated or normal IVD models.

Results

Motion segment stiffness

Motion segment stiffness decreased by 8.0% due to early stage IVD degeneration (156.7–144.2 MPa). At the same applied loads, the degenerative IVD increased motion segment damage levels by 6.6, 4.1, and 1.3% as compared to the slightly (I), moderately (II), and severely (III) damaged normal IVD models, respectively. Kyphoplasty and vertebroplasty cement augmentation of the superior VB increased the overall motion segment stiffness when compared with the damaged baseline motion segment models (Fig. 2). The third vertebroplasty repair strategy (model E), corresponding to partial fill on the periphery of the VB producing a torus- or donut-like equivalent three-dimensional geometry, and the fourth vertebroplasty strategy (model F) corresponding to a complete fill, were equally effective in increasing the degenerative IVD motion segment stiffness at each of the three damage levels. Furthermore, these were the only two repair strategies able to restore the slightly damaged (I) motion segment stiffness above undamaged levels. None of the single segment repair strategies were able to restore motion segment stiffness to undamaged levels following moderate (II) and severe (III) damage. Small differences were observed when comparing the degenerative and normal IVD motion segment repair strategies. None of the degenerative IVD models were able to achieve the same motion segment stiffness following repair as the normal IVD models. All the degenerative IVD repair models following slight damage (I) had a 2.3–2.4% reduction in motion segment stiffness as compared to the normal IVD repair models. The largest difference in motion segment modulus (stiffness) between the degenerative and normal IVD repair models was observed using model E (8.3%) and model F (8.4%) at damage level I.

Intervertebral disc

Early stage IVD degeneration resulted in an average 20.7% increase in IVD von Mises stresses and a 13.7% reduction in central endplate bulge as compared to the normal IVD motion segment model across all treatments. The third vertebroplasty treatment (model E) showed the smallest increase (19.3%) in the average IVD von Mises stresses

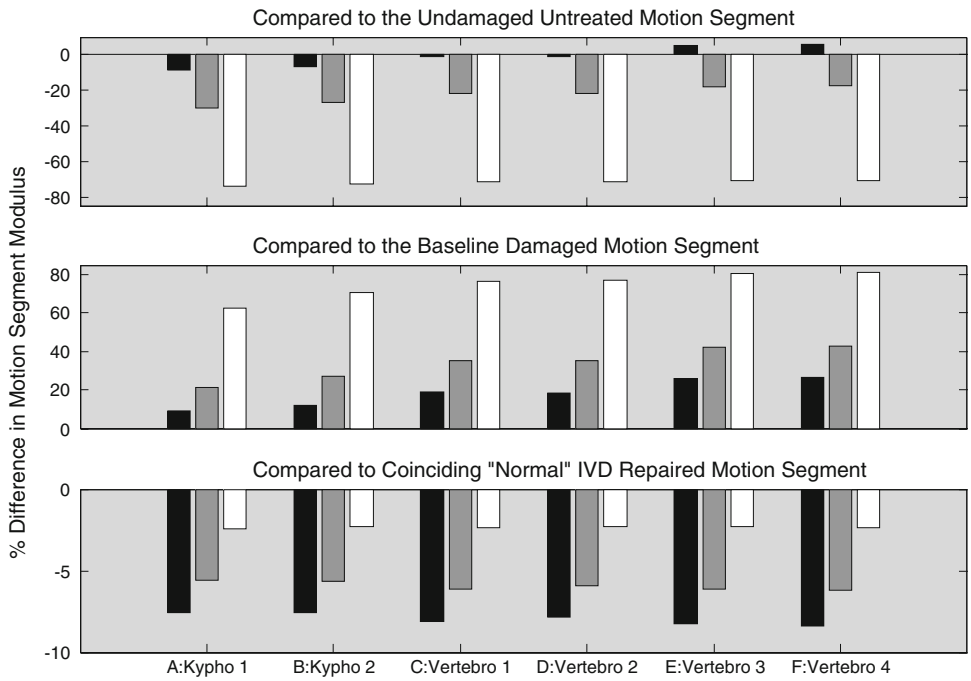

Fig. 2 Percent difference in motion segment modulus (stiffness) for each of the cement repair strategies as compared to the intact (undamaged) untreated model (*top*), baseline damage untreated models (*middle*), and normal IVD repair models. The repair effectiveness following slight (*black bar*), moderate (*gray bar*), and severe (*white bar*) bone damage is compared side-by-side for each cement augmentation treatment strategy

following repair of the slightly damaged model (I). In contrast, the highest increase (24.1%) was observed using the first kyphoplasty treatment (model A) following repair of the severely damaged model (III). A mean 2.2% increase was observed when comparing the average IVD von Mises stresses across all treatments to the IVD stresses observed in the baseline damage models. A maximum increase (8.3%) was observed when comparing the first kyphoplasty treatment (model A) at damage level III to the corresponding untreated baseline damage model. Conversely, slight reductions in the average IVD von Mises stresses (−0.3% at damage level I and −0.4% at damage level III) were found using the third vertebroplasty treatment (model E). Less than a 1% increase was observed when comparing the average degenerative IVD von Mises stresses across treatments to that of the intact untreated motion segment. A maximum stress increase of 7.6% occurred using the first kyphoplasty treatment (model A) at damage level III, and a maximum decrease of −3.0% occurred using the third vertebroplasty treatment (model E) at damage level II, as compared to the corresponding IVD of the intact untreated model.

Treated and adjacent-level vertebrae

Prior to the bone damage and cement augmentation simulations, a small reduction (1.3%) in the average tissue level von Mises stresses was observed for the superior and inferior vertebrae of the intact degenerative IVD motion segment as compared to the normal IVD motion segment. Following the damage and repair simulations, differences were once again small when comparing the average von Mises trabecular bone stresses for the superior (augmented) and inferior (untreated) VBs of the degenerative IVD motion segment models to the corresponding VB results using the normal IVD models for all the damage levels studied (Fig. 3). Both of the spherical cement augmentation treatments (models A and C) showed an increase in the average trabecular bone von Mises stresses in the treated superior VB, and a decrease in the adjacent inferior VB bone stresses, at all three damage levels for the degenerative IVD models as compared to the normal IVD models. The last three vertebroplasty repair models (models D–F) however, showed a decrease at all damage levels as compared to the normal IVD models. The torus- or donut-like repair geometry (model E) showed the largest reductions in average trabecular bone von Mises stresses for the treated (superior) VB as compared to the results from the same treatment strategy using the normal IVD motion segment models at all three damage levels. The adjacent-level (inferior) VB showed consistent reductions in average von Mises bone stresses across treatments at each of the damage levels. Percent differences in average von Mises bone stresses between the degenerative IVD repair and the baseline damage models are reported in Table 1.

Vertebral endplates

Prior to the bone damage and cement augmentation simulations, a small reduction (−2.0%) was observed in the

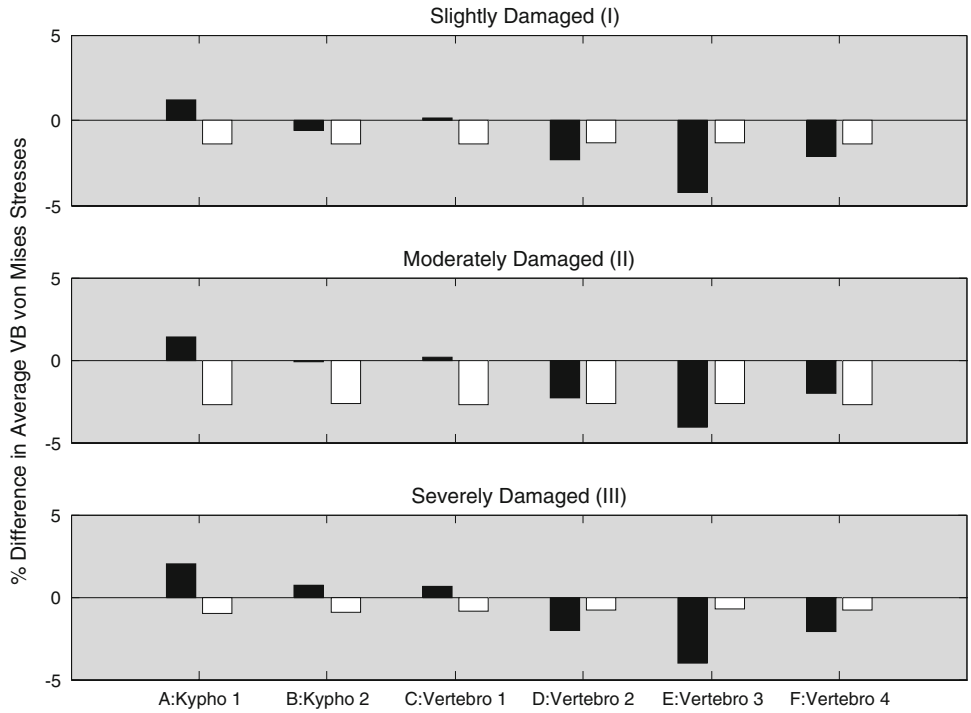

Fig. 3 Percent difference in average VB von Mises bone stresses for the treated (*black bar*) and adjacent-level (*white bar*) segments of the degenerative IVD models, as compared to the corresponding segments using the normal IVD models, for each cement augmentation treatment strategy

Table 1 Average von Mises bone stresses and corresponding percent differences for the treated (superior) and adjacent-level (inferior) segments, and for their respective endplates, as compared to the three baseline damage models

FE model	Damage model	Treated VB (superior)	Adjacent VB (inferior)	Treated VB endplate	Adjacent VB endplate
Untreated baseline damage (MPa)	I	1.222	1.220	0.795	0.782
	II	1.386	1.387	1.136	1.123
	III	1.702	1.705	1.096	1.084
A: Kypho-1 (%)	I	−4.14	0.23	52.07	0.47
	II	9.12	1.07	68.62	2.42
	III	40.80	0.40	226.10	1.37
B: Kypho-2 (%)	I	−8.21	0.14	24.45	0.29
	II	1.24	0.78	17.25	1.76
	III	10.01	0.18	82.37	0.63
C: Vertebro-1 (%)	I	−30.36	0.19	12.82	0.42
	II	−27.93	0.89	−5.43	2.03
	III	−26.92	0.18	32.93	0.61
D: Vertebro-2 (%)	I	−34.50	0.06	−6.51	0.12
	II	−32.45	0.58	−23.35	1.31
	III	−34.90	0.06	−2.99	0.19
E: Vertebro-3 (%)	I	−62.40	0.00	−34.80	−0.01
	II	−62.42	0.45	−47.30	1.03
	III	−65.70	0.02	−36.63	0.00
F: Vertebro-4 (%)	I	−65.22	0.03	−43.07	0.07
	II	−64.41	0.55	−53.71	1.24
	III	−66.87	0.04	−44.20	0.08

average von Mises stresses for the superior and inferior vertebral endplates adjacent to the degenerative IVD as compared to the normal IVD endplates. Following the damage and repair simulations, as was observed for the superior and inferior VBs, small percent differences in the average endplate von Mises stresses were found between the degenerative IVD and normal IVD models (Fig. 4). The largest variation in tissue stresses between the degenerative and normal IVD cement augmentation treatments were observed to occur at the superior (treated) VB endplate. The largest reduction (6.7%) in the average endplate stresses between the different disc conditions was found following the third vertebroplasty treatment (model E). In contrast, the endplate of the inferior VB adjacent to the IVD showed consistent reductions of 2.8, 5.8, and 2.8% in average von Mises bone stresses across treatments at damage levels I, II, and III, respectively.

Microstructural stresses

Element-by-element changes in the von Mises bone stresses following cement augmentation of the severely damaged degenerative IVD models are illustrated in the upper portion of Fig. 5. Stresses are normalized to show differences as compared to the baseline severely damaged untreated degenerative IVD model. Examination of the baseline damage normalized contour plots reveals that the addition of PMMA cement grossly altered the bone stress distributions in the augmented (superior) VB but produced much less marked changes in the adjacent-level (inferior) untreated VB. In the kyphoplasty simulations (models A and B), the trabecular bone stresses of the superior segment were notably increased above and below the cement-filled cavity and were notably decreased in regions lateral to the cement cavity. In terms of the adjacent (inferior) segment, changes in trabecular bone von Mises stresses were most marked in the vertebral endplate regions directly neighboring the degenerative IVD following each cement augmentation treatment. The observed adjacent segment load transfer, altering the endplate von Mises stress distributions, was least evident using the vertebroplasty partial fill strategy (model E) which placed the cement on the periphery of the VB producing a torus- or donut-like three-dimensional repair. In the lower part of Fig. 5 each of the cement augmentation treatments simulated using the degenerative IVD motion segment model are normalized to the same treatments using the normal IVD models. A redistribution in the von Mises bone stresses is observed in the degenerative IVD models as compared to the normal IVD models. A notable shift in stresses is generally

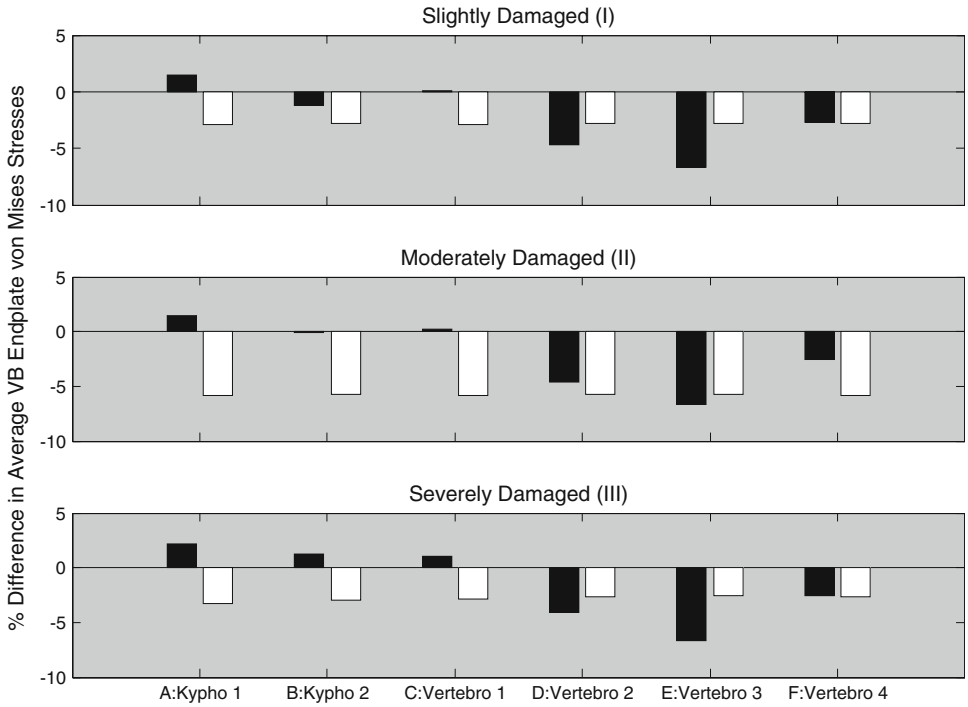

Fig. 4 Percent difference in average von Mises bone stresses for the inferior endplate (*black bar*) of the treated segment and the superior endplate (*white bar*) of the adjacent-level segment. Differences shown are between the degenerative IVD and normal IVD models following repair of the slightly (*top*), moderately (*middle*), and severely (*bottom*) damaged microstructural FE models using each of the cement augmentation treatment strategies

observed in both the treated (superior) and adjacent segment endplates. This shift is represented by a decrease in bone stresses at the central endplate region (i.e., the endplate area which surrounded the IVD nucleus in the normal IVD repair models), and an increase in the peripheral endplate regions above and below the IVD annulus. This shift in von Mises stresses toward the periphery of the endplates is most pronounced in the third (model E) and fourth (model F) vertebroplasty treatments. In contrast, the superior VB endplate overlying the degenerative IVD for the first kyphoplasty treatment (model A) showed a homogeneous increase in von Mises bone stresses as compared to the same treatment strategy in the normal IVD model.

Discussion

This study aimed to numerically evaluate the effectiveness of six different cement augmentation strategies in repairing a slightly, moderately, and severely damaged degenerative IVD motion segment. The novel results from this study come from directly comparing the same compressive loading and augmentation strategies between normal and degenerative IVD motion segment models.

Overall, small differences were observed in motion segment stiffness and average stresses between the degenerative and normal IVD motion segment repair models. The small differences found in motion segment stiffness are mostly due to the increased damage levels found in the degenerative IVD damage models. Normalizing to the initial damage stiffness, we see an average 1.5% (1.0–2.2%) difference in stiffness between the degenerative and normal IVD models. Although small differences were also found in the average von Mises bone stresses between the two disc models, a reduction in endplate bulge and a redistribution in the microstructural tissue stresses across both endplates and in the treated (superior) segment was observed. In agreement with the literature [31], degeneration of the IVD in our models resulted in a stress shift toward the periphery of the trabecular core.

The results from this study confirm previous findings suggesting that vertebroplasty repair may be more effective than kyphoplasty in increasing motion segment stiffness, reducing treated segment bone stresses, and minimizing load transfer to the adjacent-level following bone damage [12] (see Fig. 5). The models however do not simulate height restoration observed in kyphoplasty or variations in sagittal alignment with progressive microfractures. Variations in sagittal alignment before and after cement augmentation may alter the observed stress distributions from this study and have been shown to be related to adjacent-level VCF [32]. Furthermore, the results from these analyses are limited to uniform compressive loading. Using combined loading, disc degeneration has been shown to alter IVD stress peaks with disc degeneration in a flexed posture [24]. The numerical bone microdamage scheme in conjunction with a microstructural FE approach as presented in this study however, has been shown to reproduce the experimental

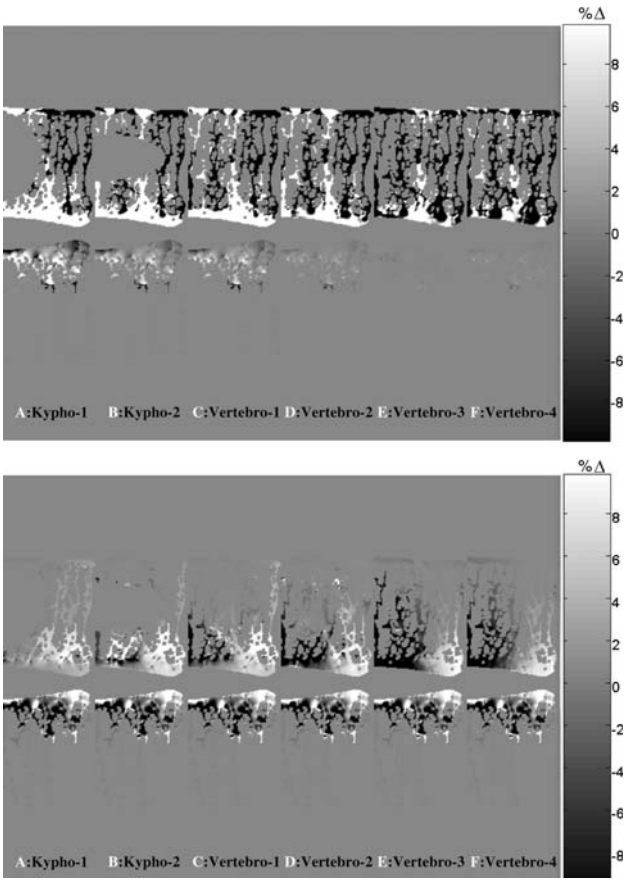

Fig. 5 Element-by-element percent changes in the microstructural bone tissue von Mises stress distributions for each of the six cement augmentation models (*A–F*) as compared with the baseline maximally damaged (III) models (*top*), and corresponding normal IVD repair models (*bottom*). von Mises stress changes in the IVD and PMMA elements are not shown (arbitrarily assigned to 0%)

nonlinear stress–strain behavior of human vertebrae subjected to compressive loading [15, 16, 18, 19].

The IVD degeneration model is limited in that it does not capture disc height reduction and/or increased endplate curvature as may be seen during aging. Furthermore it does not simulate the multiphase behavioral changes occurring within the IVD. The degenerative model is however in very close agreement with previous experimental and numerical studies reporting an initial reduction in motion segment compressive stiffness following early stage IVD degeneration [4, 5, 31]. In addition, our reported reduction in endplate bulge and increase in IVD von Mises stress due to the reduction in the incompressibility characteristics of the nucleus following IVD degeneration is in agreement with previous findings [13, 33].

The results presented are consistent with previous experimental and numerical findings [2, 9, 12, 36] reporting the inability of a single segment cement augmentation to restoring moderately and severely damaged motion segment compressive stiffness back to, or above intact levels. In extending our findings to the clinic, our study is limited in that the cement augmentation strategies presented are idealized and not currently practical to perform. Such analyses evaluating different theoretical repair strategies however, do provide a controlled means to further evaluate and increase our understanding of the underlying biomechanics in cement augmentation repair. The torus- or donut-like cement augmentation geometry (model E) was most effective in treating the damaged degenerative IVD motion segment models. This strategy was able to restore the motion segment stiffness above intact levels following slight bone damage (I), and showed the largest reduction (although small) in the average IVD von Mises stresses as compared to both the intact and baseline damage untreated models. In addition, this strategy proved to be the most advantageous in treating the degenerative IVD models by showing larger reductions in the average von Mises bone stresses for the VBs and their coinciding endplates, as compared to the normal IVD models. In contrast, the spherical kyphoplasty treatment (model A) was the least effective strategy. The microstructural tissue stress results from this strategy agreed with previous findings showing increased stress concentrations in the trabecular structure above and below the cement [12, 17]. In addition, this strategy had the highest increase in average stresses at the endplates and the IVD as compared to the intact and baseline damage untreated models. Biomechanically, if such a partial strategy is to be used, the cement should at least extend to the VB endplates providing an upright pillar-like support and thus reducing the higher stress concentrations observed in the load transferring trabeculae above and below the cement bolus [17]. The findings from this study however, are based on relative comparisons of a single motion segment, making it difficult to generalize with confidence to other spines and spinal levels. Future research should aim to further evaluate and develop ways of clinically reproducing the effective donut-like idealized geometry (model E) provided that special emphasis is placed on minimizing the increased likelihood of cement leakage from such a peripheral treatment strategy.

In summary, our analyses suggest that early stage disc degeneration does not have an appreciable affect in motion segment stiffness, and average von Mises stresses in the treated and adjacent-level segments following vertebroplasty and kyphoplasty. Furthermore, placing bone cement in the periphery (model E) of the damaged VB in a degenerative IVD motion segment, minimizes load transfer, and may reduce the likelihood of adjacent-level VCFs.

References

1. Baroud G, Nemes J, Heini P, Steffen T (2003) Load shift of the intervertebral disc after a vertebroplasty: a finite-element study. Eur Spine J 12:421–426. doi:10.1007/s00586-002-0512-9
2. Belkoff SM, Mathis JM, Jasper LE, Deramond H (2001) The biomechanics of vertebroplasty. The effect of cement volume on mechanical behavior. Spine 26:1537–1541. doi:10.1097/00007632-200107150-00007
3. Berlemann U, Ferguson SJ, Nolte LP, Heini PF (2002) Adjacent vertebral failure after vertebroplasty. A biomechanical investigation. J Bone Joint Surg Br 84:748–752. doi:10.1302/0301-620X.84B5.11841
4. Brown MD, Holmes DC, Heiner AD (2002) Measurement of cadaver lumbar spine motion segment stiffness. Spine 27:918–922. doi:10.1097/00007632-200205010-00006
5. Brown MD, Holmes DC, Heiner AD, Wehman KF (2002) Intraoperative measurement of lumbar spine motion segment stiffness. Spine 27:954–958. doi:10.1097/00007632-200205010-00014
6. Fribourg D, Tang C, Sra P, Delamarter R, Bae H (2004) Incidence of subsequent vertebral fracture after kyphoplasty. Spine 29:2270–2276. doi:10.1097/01.brs.0000142469.41565.2a
7. Garfin SR, Yuan HA, Reiley MA (2001) New technologies in spine: kyphoplasty and vertebroplasty for the treatment of painful osteoporotic compression fractures. Spine 26:1511–1515. doi:10.1097/00007632-200107150-00002
8. Guo LX, Teo EC (2006) Influence prediction of injury and vibration on adjacent components of spine using finite element methods. J Spinal Disord Tech 19:118–124. doi:10.1097/01.bsd.0000191527.96464.9c
9. Kayanja MM, Togawa D, Lieberman IH (2005) Biomechanical changes after the augmentation of experimental osteoporotic vertebral compression fractures in the cadaveric thoracic spine. Spine J 5:55–63
10. Keller TS, Holm SH, Hansson TH, Spengler DM (1990) 1990 Volvo Award in experimental studies. The dependence of intervertebral disc mechanical properties on physiologic conditions. Spine 15:751–761. doi:10.1097/00007632-199008010-00004
11. Keller TS, Kosmopoulos V, Liebschner MA (2002) Modeling of bone loss and fracture in osteoporosis. In: Gunzburg R, Szpalski M (eds) Vertebral osteoporotic compression fractures. Lippincott-Raven, Philadelphia, pp 35–50
12. Keller TS, Kosmopoulos V, Lieberman IH (2005) Vertebroplasty and kyphoplasty affect vertebral motion segment stiffness and stress distributions: a microstructural finite-element study. Spine 30:1258–1265. doi:10.1097/01.brs.0000163882.27413.01
13. Kim YE, Goel VK, Weinstein JN, Lim TH (1991) Effect of disc degeneration at one level on the adjacent level in axial mode. Spine 16:331–335. doi:10.1097/00007632-199103000-00013
14. Kim SH, Kang HS, Choi JA, Ahn JM (2004) Risk factors of new compression fractures in adjacent vertebrae after percutaneous vertebroplasty. Acta Radiol 45:440–445. doi:10.1080/02841850410005615
15. Kosmopoulos V, Keller TS (2003) Bone microdamage and repair simulations using an elastoplastic numerical scheme. In: Hamza MH (ed) Proceedings of the twelfth international association of science and technology for development conference on applied simulation and modelling. ACTA Press, Calgary, pp 319–324
16. Kosmopoulos V, Keller TS (2003) Finite element modeling of trabecular bone damage. Comput Methods Biomech Biomed Engin 6:209–216. doi:10.1080/1025584031000149089
17. Kosmopoulos V, Keller TS (2004) Damage-based finite-element vertebroplasty simulations. Eur Spine J 13:617–625. doi:10.1007/s00586-003-0651-7
18. Kosmopoulos V, Keller TS (2008) Predicting trabecular bone microdamage initiation and accumulation using a non-linear perfect damage model. Med Eng Phys 30:725–732. doi:10.1016/j.medengphy.2007.02.011
19. Kosmopoulos V, Keller TS, Baroud G, Steffen T (2003) Experimental and numerical simulation of microdamage and failure of thoracic vertebral trabecular bone. Trans Orthop Res Soc 28:453
20. Kosmopoulos V, Schizas C, Keller TS (2008) Modeling the onset and propagation of trabecular bone microdamage during low-cycle fatigue. J Biomech 41:515–522. doi:10.1016/j.jbiomech.2007.10.020
21. Ledlie JT, Renfro M (2003) Balloon kyphoplasty: one-year outcomes in vertebral body height restoration, chronic pain, and activity levels. J Neurosurg 98:36–42
22. Lieberman IH, Dudeney S, Reinhardt MK, Bell G (2001) Initial outcome and efficacy of "kyphoplasty" in the treatment of painful osteoporotic vertebral compression fractures. Spine 26:1631–1638. doi:10.1097/00007632-200107150-00026 see comment
23. Liebschner MA, Rosenberg WS, Keaveny TM (2001) Effects of bone cement volume and distribution on vertebral stiffness after vertebroplasty. Spine 26:1547–1554. doi:10.1097/00007632-200107150-00009
24. Luo J, Skrzypiec DM, Pollintine P, Adams MA, Annesley-Williams DJ, Dolan P (2007) Mechanical efficacy of vertebroplasty: influence of cement type, BMD, fracture severity, and disc degeneration. Bone 40:1110–1119. doi:10.1016/j.bone.2006.11.021
25. Majd ME, Farley S, Holt RT (2005) Preliminary outcomes and efficacy of the first 360 consecutive kyphoplasties for the treatment of painful osteoporotic vertebral compression fractures. Spine J 5:244–255
26. McKiernan F, Faciszewski T, Jensen R (2003) Reporting height restoration in vertebral compression fractures. Spine 28:2517–2521. doi:10.1097/01.BRS.0000092424.29886.C9
27. Mehbod A, Aunoble S, Le Huec JC (2003) Vertebroplasty for osteoporotic spine fracture: prevention and treatment. Eur Spine J 12(Suppl 2):S155–S162. doi:10.1007/s00586-003-0607-y Review. 64 refs
28. Phillips FM, Todd WF, Lieberman I, Campbell-Hupp M (2002) An in vivo comparison of the potential for extravertebral cement leak after vertebroplasty and kyphoplasty. Spine 27:2173–2178. doi:10.1097/00007632-200210010-00018
29. Phillips FM, Ho E, Campbell-Hupp M, McNally T, Todd WF, Gupta P (2003) Early radiographic and clinical results of balloon kyphoplasty for the treatment of osteoporotic vertebral compression fractures. Spine 28:2260–2265. doi:10.1097/01.BRS.0000085092.84097.7B
30. Polikeit A, Nolte LP, Ferguson SJ (2003) The effect of cement augmentation on the load transfer in an osteoporotic functional spinal unit: finite-element analysis. Spine 28:991–996. doi:10.1097/00007632-200305150-00006
31. Polikeit A, Nolte LP, Ferguson SJ (2004) Simulated influence of osteoporosis and disc degeneration on the load transfer in a lumbar functional spinal unit. J Biomech 37:1061–1069. doi:10.1016/j.jbiomech.2003.11.018
32. Rohlmann A, Zander T, Bergmann G (2006) Spinal loads after osteoporotic vertebral fractures treated by vertebroplasty or kyphoplasty. Eur Spine J 15:1255–1264. doi:10.1007/s00586-005-0018-3
33. Rohlmann A, Zander T, Schmidt H, Wilke HJ, Bergmann G (2006) Analysis of the influence of disc degeneration on the mechanical behaviour of a lumbar motion segment using the finite element method. J Biomech 39:2484–2490. doi:10.1016/j.jbiomech.2005.07.026
34. Saxena R, Keller TS (1999) Computer modeling for evaluating trabecular bone mechanics. In: An YH, Draughn RA (eds)

Mechanical testing of bone and the bone-implant interface. CRC, Boca Raton, pp 407–436
35. Shirazi-Adl SA, Shrivastava SC, Ahmed AM (1984) Stress analysis of the lumbar disc-body unit in compression. A three-dimensional nonlinear finite element study. Spine 9:120–134. doi:10.1097/00007632-198403000-00003
36. Tomita S, Kin A, Yazu M, Abe M (2003) Biomechanical evaluation of kyphoplasty and vertebroplasty with calcium phosphate cement in a simulated osteoporotic compression fracture. J Orthop Sci 8:192–197. doi:10.1007/s007760300032
37. Villarraga ML, Bellezza AJ, Harrigan TP, Cripton PA, Kurtz SM, Edidin AA (2005) The biomechanical effects of kyphoplasty on treated and adjacent nontreated vertebral bodies. J Spinal Disord Tech 18:84–91. doi:10.1097/01.bsd.0000138694.56012.ce